Progress In Electromagnetics Research, Vol. 161, 11–18, 2018

Exploratory Study on Light-Sheet Based Three-Dimensional Surface Topography

Fuhong Cai[1], Jie Chen[1], Chunling Zhou[2], Xuan Zhu[1], and Sailing He[2, *]

Abstract—Light-sheet microscopy has attracted considerable attention because it is a fluorescence imaging technique with rapid optical sectioning capability for transparent samples. In this study, we report a new application based on light-sheet microscopy for exploratory investigation of three-dimensional surface topography of opaque objects. Instead of using inelastic scattering fluorescent signals, our method utilizes the elastic scattering of light from the surface of opaque samples, which are illuminated by a light sheet generated by a cylindrical lens. Through a simple structural modification by removing the fluorescent filter, the orthogonal imaging module can capture the elastically-scattered image. As the opaque object is scanned by a motorized stage, the light-sheet microscope acquires a series of sectional images, which can be stitched into a three-dimensional surface topography image. This method also offers the opportunity to visualize a 3D fingerprint at micron-level resolution. Therefore, this technique may be used in industry and the biomedical field for the measurement of surface microstructure. To our best knowledge, this is the first time a light-sheet microscopy is utilized to perform surface topography measurement.

1. INTRODUCTION

Optical imaging systems have become essential tools in the fields of biomedical and industrial applications. Over the past two decades, confocal and two-photon laser scanning microscopes have been widely used in three-dimensional (3D) *in-vivo* molecular imaging and *in-situ* observation of microstructure of industrial products [1–5]. Compared with traditional confocal and two-photon microscopy, line detection techniques provide a fast imaging method for spectrally and spatially resolved images [6–11]. Line detection techniques have also found wide applications in chemistry [6] and food inspection [10, 11]. Recently, the light-sheet microscopy (LSM) technique, which illuminates a transparent sample with a thin sheet of laser light and images the sample orthogonally, facilitates rapid volumetric imaging [12–17]. The thin sheet of laser light can be static, generated by a cylindrical lens [12], or virtual, generated by a fast-scanning galvo-mirror [13, 14]. A fluorescent filter installed before the camera is utilized to block the excited laser light and improve the signal to noise ratio (SNR). Due to its excellent SNR, low photo-toxicity, and high sectional imaging speed, LSM has become a technique of choice for biologists. Additionally, to study biological processes at super-resolution levels, light sheet–based technologies have been utilized as optical imaging platforms for structured illumination microscopy (SIM) and stochastic optical reconstruction microscopy (STORM) [18–21]. In all of the above cases, LSM relies on fluorescent light emitted from bio-samples to form a sectional image.

There has been remarkable research on 3D morphology recently [22–25]. In our study, we seek to exploit elastic scattering to implement 3D surface morphology measurement of opaque samples based on modified LSM in which the fluorescent filter is removed. Because of the good coherence characteristics

Received 27 January 2018, Accepted 3 March 2018, Scheduled 5 March 2018

* Corresponding author: Sailing He (sailing@kth.se).

[1] College of Mechanical and Electrical Engineering, Hainan University, Hainan 570228, China. [2] Centre for Optical and Electromagnetic Research, State Key Laboratory for Modern Optical Instrumentation, Zhejiang University; Joint Research Center of Photonics of the Royal Institute of Technology, Lund University and Zhejiang University(JORCEP), Hangzhou 310058, China.

of laser light, there is inherent speckle noise in the images. Even so, we can still generate 3D surface morphology results based on the scanning images. In this paper, we will describe the feasibility of 3D morphology measurements for a metal screw, electronic chip components, and a fingerprint.

2. OPTICAL SETUP

The developed setup is on a traditional microscope, as shown in Fig. 1(a). This system contains two major modules: the illumination module and the imaging module. In the illumination module, a light sheet is created using a cylindrical lens to focus a collimated 532 nm laser beam. The collimated laser beam, with finite beam size, is focused in only one direction by the cylindrical lens, near whose focal point a light sheet can be generated. Herein, only one optical section of the sample is illuminated. The imaging module is perpendicular to the illumination module such that the light sheet on the sample is reflected or backscattered from the surface of sample. The reflected or backscattered light can be captured by a 4X microscope objective in the imaging module. The reflected or backscattered light then passes through a tube lens and is focused on a CMOS chip. Thus, we can acquire a photo for the surface profile of one section of the sample.

To demonstrate the suitability of our system for opaque samples, we first applied LSM to image a glass slide, whose thickness is 1.14 mm. As shown in Fig. 1(c), the reflected light from the top and bottom layers of the glass slide formed two vertical lines From the view point of the imaging module, the distance between the reflected rays from the top and bottom layers was 833.35 μm (see Fig. 1(c)). We can establish the quantitative accuracy by calculating the thickness of the glass slide. Based on the Snell's law and theory of plane geometry, the thickness is $(833.35\sin\Theta_1/\ \tan\Theta_2)\mu m = 1117\,\mu m$. Herein, Θ_1 and Θ_2 are the incidence angle (45 degree) and refraction angle (27.80 degree) respectively. The refractive index was about 1.5163. We also used a Vernier caliper to measure the thickness of glass slide, and the result was 1.14 mm. Therefore, the measuring error was about $(1.14–1.117)/1.14 = 1.64\%$, which is mainly caused by speckle noise. It should be noted that the speckle noise makes the contour profile thicker, resulting in some error for surface topography measurement.

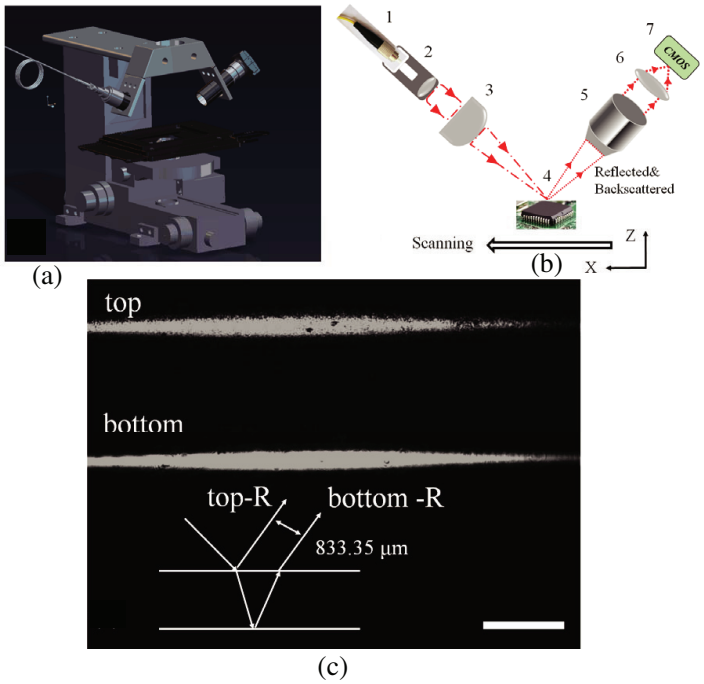

Figure 1. (a) Prototype of the light-sheet based 3D surface topography; (b) Schematic diagram of the light-sheet based 3D surface topography. 1: Single mode fiber. 2: Fiber collimator. 3: cylindrical lens. 4: sample. 5: objective. 6: tube lens. 7: CMOS sensor. (c) Imaging result for a glass slide. Scale Bar: 500 μm.

3. RESULTS AND DISCUSSION

In this section, using our LSM system, we performed three scanning experiments for a metal screw, an electronic chip, and a fingerprint. In each experiment, an exploratory image processing method was used to overcome the influence of speckle noise.

3.1. Surface Topography Measurement for Metal Screw

With our LSM system, we scanned an M6 metal screw, and 236 sectional images were acquired. Three sectional images, i.e., the 1th, the 120th, and the 236th, are shown in Fig. 2(a)–(c). We select the 120th image as a representative sample image to demonstrate how to extract the contour in a sectional image. Due to speckle noise, part of the image is generally buried in random noise. We first applied '*imguidedfilter*' in Matlab software to perform imaging smoothing. The filtered result for the 120th image is shown in Fig. 2(d), whose inset shows an intensity line profile for the dotted line region. Observing this intensity line profile, we found that to the left of the boundary spot, the intensity value was almost zero. Next, we developed an image processing method to find the boundary spot of the intensity line profile. The processing steps are shown as follows:

1. Load one filtered image into the Matlab workspace, converting the image to a gray matrix named '*Img*' (960×1280).
2. Set the window width and threshold value to 20 and 120, respectively.
3. Loop i from 1 to 960, for each horizontal line, creating a vector $hor\_prol = Img(i,:)$ in Matlab. '*hor_prol*' represents the intensity line profile.

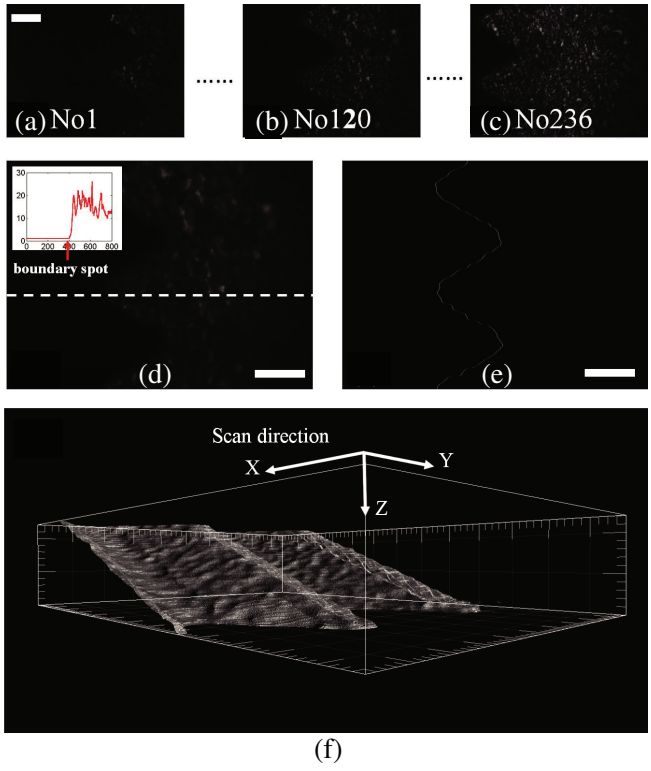

Figure 2. Light-sheet microscopy scan of an M6 metal screw, obtaining 236 sectional images. The 1th, the 120th, and the 236th images are selected and shown in (a)–(c). After smoothing, filtering, and edge detection for the 120th image, the filtered and contoured images are shown in (d) and (e), respectively. (f) After image processing, all 236 contoured images are stitched to become a 3D topography result by Imaris software. Scale Bar: 500 µm.

4. Loop j from 1 to 1280-20, sum $hor\_prol(j : j + 20)$. If the result is larger than threshold value (120), break the loop. The boundary spot is the current j value in this line.

We applied the above method to process all of the filtered images and acquired 236 contour images. Fig. 2(e) shows the 120th contour image. We imported these contour images into Imaris software, which automatically generated a 3D surface topography of the metal screw, as shown in Fig. 2(f). It is important to note that our image processing method is still not yet optimized in terms of the localization accuracy of the boundary spot. Observing Fig. 2(d), the contour image should be a smooth sawtooth curve; however, there are small rises and falls in the processed result, as shown in Fig. 2(e) and Fig. 2(f).

3.2. Surface Topography Measurement for Electronic Chip

We also performed a similar scanning experiment on an electronic chip, and the results are shown in Fig. 3. Here, there are 348 sectional images in total. We selected the 185th image to explain how to extract the contour image. Similarly, we utilized the '*imguidedfilter*' function to smooth the image. The filtered result is shown in Fig. 3(d). Next, the following steps were utilized to process the filtered image:

1. Load one filtered image into the workspace of Matlab, converting the image to a gray matrix named '*Img*' (960×1280).

2. Loop j from 1 to 1280 for each vertical line, creating a vector $ver\_prol = Img(i,:)$ in Matlab and a vector id=[1:960], where '*ver_prol*' represents the intensity line profile.

3. Use the following Matlab script command: '*floor(sum(ver_prol.*id)/ sum (ver_prol))*' to calculate the centroid of the intensity line profile.

The processed result for Fig. 3(d) is shown in Fig. 3(e). Repeating the above processing method for all sectional images, we acquired 348 contour images. The 3D surface topography, reconstructed by Imaris software, is shown in Fig. 3(f).

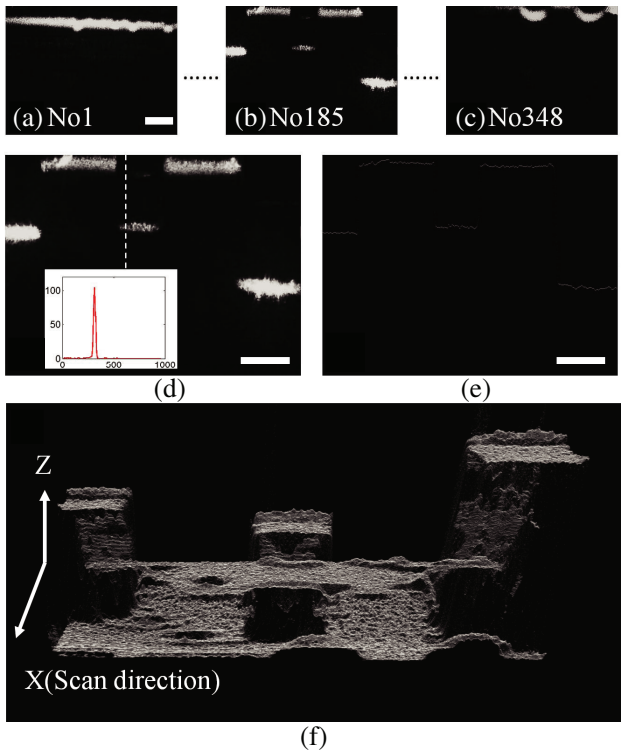

Figure 3. (a) Another similar scan was performed on a chip. The 1th, 185th, and 348th images are selected and shown in (a)–(c). After smoothing, filtering, and center detection for the 185th image, the filtered and contoured images are shown in (d) and (e) respectively. (f) After image processing, all 348 contour images are stitched to become a 3D topography result by Imaris software. Scale Bar: 500 μm.

4. SURFACE TOPOGRAPHY MEASUREMENT FOR FINGERPRINT

In this section, we demonstrate the potential of our system for bio-imaging. Herein, the imaging sample was a fingerprint. However, we cannot use a motor stage to move a finger, and we have not yet developed a motorized LSM system. Therefore, during the scanning experiment, the first author moved his finger by himself. We understood that this manual scanning would cause a large error in the result; however, we believe that the results can still be used to demonstrate the feasibility of 3D morphology measurements for fingerprint. There were 100 images obtained from the scanning experiment. Since the surface of the finger presented most optical intensity, we utilized the '*im2bw*' function in Matlab to extract the surface contour [26, 27]. Three processed results are shown in Figs. 4(d)–(f). The 3D surface topography is shown in Fig. 4(g).

We then applied the LSM to record a video of a moving finger. We presented three snapshots (1280×960) of the video in Figs. 5(a)–(c). During the experiment, a finger approached a glass slide. The raised and lowered skin (ridges and furrows) of the fingerprint can be observed in these snapshots. Our CMOS camera provides a frame rate up to 14 frames per second With a better camera, a higher frame rate could be achieved.

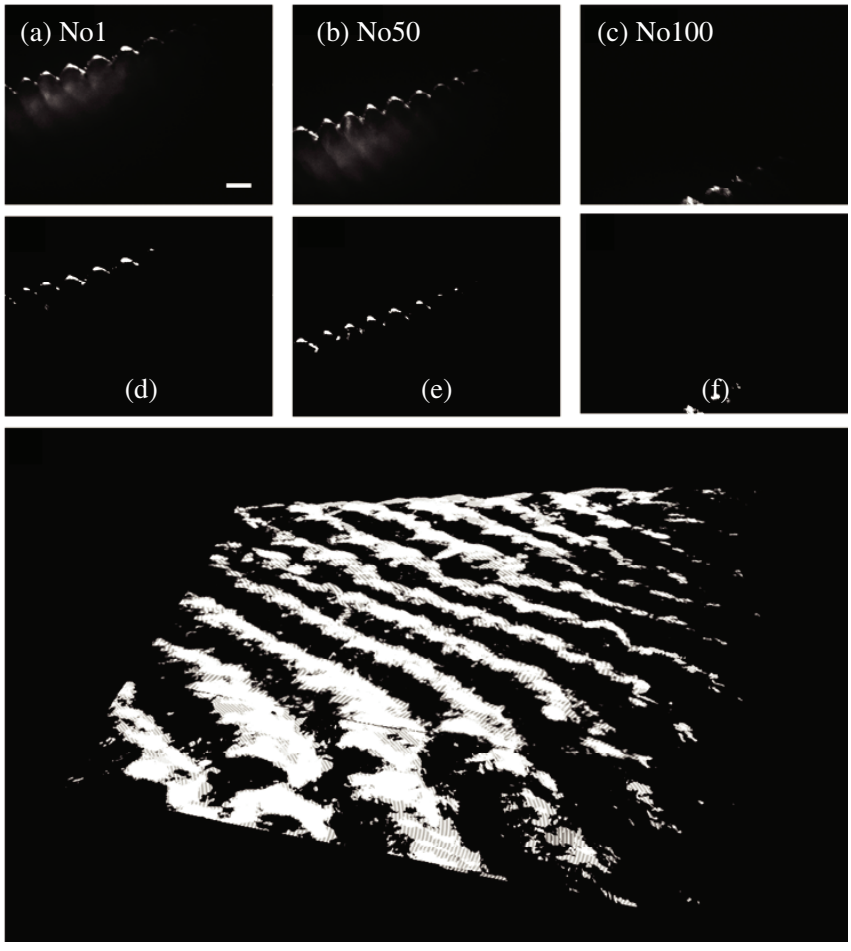

Figure 4. The results of *in-vivo* scanning of a fingerprint. One hundred experimental images were obtained; the 1th, 50th and the 100th images are shown in (a)–(c). The corresponding binary images are shown in (d)–(f). (f) 3D topography result for fingerprint. Scale Bar: 500 µm.

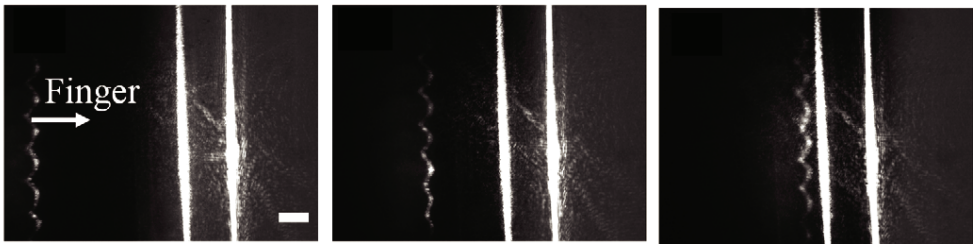

Figure 5. The results of *in-vivo* imaging of a fingerprint. (a)–(c) Three snapshots from a video, which recorded a finger approaching a glass slide. Scale Bar: 500 μm.

5. CONCLUSION

In this study, we have designed a labelfree, light sheet based, three-dimensional surface topography system. We have demonstrated the rapid sectional imaging properties of our system. The thickness of the glass slide could be calculated accurately based on the sectional image. Therefore, the system has the ability to measure accurately. We have presented three scanning experiments using our system, and the 3D topography results for a metal screw, an electronic chip, and a fingerprint are obtained. For our setup, we have also performed an evaluation experiment to record the dynamic process of a finger approaching a glass slide. At present, the image quality is mainly interfered by the speckle noise. To reduce the speckle pattern of the continuous-wave laser, one can use a supercontinuum laser as the illumination source. In this way, the speckle noise can be reduced due to the wide bandwidth of the supercontinuum laser. We can also utilize our system to scan a larger object by increasing the travel length of the motorized stage. Combining some phase contrast imaging method, this system may be utilized in 3D imaging of transparent cells.

With this optical design, the integration of other brands and models of optical devices will be straightforward. For example, our system can be applied to study surface structures at the nano-scale by using a UV laser and a high numerical aperture objective lens. This system also has the potential of being installed underwater to monitor plankton. In addition, our system can be utilized for transparent samples of several layers, as shown in Fig. 1. Since biological tissue scatters few photons at short-wave infrared bands (e.g., 1310 nm and 1680 nm) [28, 29], this system may have the potential to become a three-dimensional imaging tool for skin or human crystalline lenses using short-wave infrared devices.

ACKNOWLEDGMENT

This work is partially supported by the National Natural Science Foundation of China (11621101), Natural Science Foundation of Hainan Province (617022), Scientific research fund of Hainan University (kyqd1653) and Changshu innovative and entrepreneurship fund (CSRC1535).

The authors would like to thank Dr. Xianliang Zheng for discussion in the experiment.

REFERENCES

1. Pawley, J. B. (ed.), *Handbook of Biological Confocal Microscopy*, 3rd Edition, Springer, New York, 2006.
2. Helmchen, F. and W. Denk, "Deep tissue two-photon microscopy," *Nature methods*, Vol. 2, 932–940, 2005.
3. Li, J., F. Cai, Y. Dong, Z. Zhu, X. Sun, H. Zhang, and S. He, "A portable confocal hyperspectral microscope without any scan or tube lens and its application in fluorescence and Raman spectral imaging," *Optics Communications*, Vol. 392, 1–6, 2017.
4. Tabaksblat, R., R. Meier, and B. Kip, "Confocal Raman microspectroscopy: theory and application to thin polymer samples," *Applied Spectroscopy*, Vol. 46, 60–68, 1992.

5. Knoester, A. and G. Brakenhoff, "Applications of confocal microscopy in industrial solid materials: Some examples and a first evaluation," *Journal of Microscopy*, Vol. 157, 105–113, 1990.
6. Qin, J., K. Chao, and M. S. Kim, "A line-scan hyperspectral system for high-throughput Raman chemical imaging," *Applied spectroscopy*, Vol. 68, 692–695, 2014.
7. Cai, F., W. Lu, W. Shi, and S. He, "A mobile device-based imaging spectrometer for environmental monitoring by attaching a lightweight small module to a commercial digital camera," *Scientific reports*, Vol. 7, 15602, 2017.
8. Cai, F., D. Wang, M. Zhu, and S. He, "Pencil-like imaging spectrometer for bio-samples sensing," *Biomedical Optics Express*, Vol. 8, 5427–5436, 2007.
9. Sinclair, M., J. Timlin, D. Haaland, and M. Werner-Washburne, "Design, construction, characterization, and application of a hyperspectral microarray scanner," *Applied Optics*, Vol. 43, 2079–2088, 2004.
10. Nakariyakula, S. and D. Casasentb, "Fast feature selection algorithm for poultry skin tumor detection in hyperspectral data," *Journal of Food Engineering*, Vol. 94, 358–365, 2009.
11. Cai, F., R. Tang, S. Wang, and S. He, "A compact line-detection spectrometer with a Powell lens," *Optik-International Journal for Light and Electron Optics*, Vol. 155, 267–272, 2018.
12. Biggs, K. B., K. M. Balss, and C. A. Maryanoff, "High-resolution three-dimensional imaging of large specimens with light sheet–based microscopy," *Nature Methods*, Vol. 4, 311–313, 2007.
13. Keller, P. J., A. D. Schmidt, J. Wittbrodt, and E. H. Stelzer, "Reconstruction of zebrafish early embryonic development by scanned light sheet microscopy," *Science*, Vol. 322, 1065–1069, 2008.
14. Truong, T., W. Supatto, D. Koos, J. Choi, and S. Fraser, "Deep and fast live imaging with two-photon scanned light-sheet microscopy," *Nature Methods*, Vol. 8, 757–760, 2011.
15. Xu, D., W. Zhou, and L. Peng, "Three-dimensional live multi-label light-sheet imaging with synchronous excitation-multiplexed structured illumination," *Optics Express*, Vol. 25, 31159–31173, 2017.
16. Cao, Z., C. Zhai, J. Li, F. Xian and S. Pei, "Light sheet based on one-dimensional Airy beam generated by single cylindrical lens," *Optics Communications*, Vol. 393, 11–16, 2017.
17. Cao, Z. and C. Zhai, " Scattering of one-dimensional Airy beam light sheet with finite energy by a sphere," *Applied Optics*, Vol. 56, 3491–3496, 2017.
18. Gustafsson, M., "Surpassing the lateral resolution limit by a factor of two using structured illumination microscopy," *Journal of Microscopy*, Vol. 198, 82–87, 2000.
19. Keller, P., A. Schmidt, A. Santella, K. Khairy, Z. Bao, J. Wittbrodt, and E. Stelzer, "Fast, high-contrast imaging of animal development with scanned light sheet-based structured-illumination microscopy," *Nature Methods*, Vol. 7, 637–642, 2010.
20. Rust, M., M. and X. Zhuang, "Sub-diffraction-limit imaging by stochastic optical reconstruction microscopy (STORM)," *Nature Methods*, Vol. 3, 793–796, 2006.
21. Hu, Y., M. Zimmerley, Y. Li, R. Watters, and H. Cang, "Single-molecule super-resolution light-sheet microscopy," *Chem. Phys. Chem.*, Vol. 15, 577–586, 2014.
22. Lei, Z., X. Liu, L. Zhao, L. Chen, Q. Li, T. Yuan, and W. Lu, "A novel 3D stitching method for WLI based large range surface topography measurement," *Optics Communications*, Vol. 359, 435–447, 2016.
23. Lédl, V., P. Psota, F. Kaván, O. Matoušek, and P. Mokrý "Surface topography measurement by frequency sweeping digital holography," *Applied Optics*, Vol. 56, 7808–7814, 2017.
24. Zhang, T. F. and X. Jiang, "Surface topography acquisition method for double-sided near-right-angle structured surfaces based on dual-probe wavelength scanning interferometry," *Optics Express*, Vol. 25, 24148–24156, 2017.
25. Sun, M., J. Birkenfeld, A. Castro, S. Ortiz, and S. Marcos, "OCT 3-D surface topography of isolated human crystalline lenses," *Biomedical Optics Express*, Vol. 5, 3547–3561, 2014.
26. Wang, L., S. Jacques, and L. Zheng, "MCML — Monte Carlo modeling of light transport in multi-layered tissues," *Computer Methods and Programs in Biomedicine*, Vol. 47, 131–146, 1995.

27. Cai, F. and W. Lu, "A dynamic accuracy estimation for gpu-based monte carlo simulation in tissue optics," *Current Optics and Photonics*, Vol. 1, 551–555, 2017.
28. Hong, G. S., S. Diao, J. L. Chang, A. L. Antaris, C. X. Chen, B. Zhang, S. Zhao, D. N. Atochin, P. L. Huang, K. I. Andreasson, C. J. Kuo, and H. J. Dai, "Through-skull fluorescence imaging of the brain in a new near-infrared window," *Nature Photonics*, Vol. 8, 723–730, 2014.
29. Cai, F., J. Yu, J. Qian, Y. Wang, Z, Chen, J. Huang, Z. Ye, and S. He, "Use of tunable second-harmonic signal from KNbO3 nanoneedles to find optimal wavelength for deep-tissue imaging," *Laser & Photonics Reviews*, Vol. 8, 865–874, 2014.